

Localization Uncertainty Constrained Lateral PID Control with Aids of Fuzzy Logic Considering LiDAR NDT Matching Error *

Sai Hu, Yin-Chiu Kan, and Li-Ta Hsu **

*Interdisciplinary Division of Aeronautical and Aviation Engineering,
The Hong Kong Polytechnic University, Hong Kong*

ABSTRACT

Localization and control are two key parts of autonomous driving. Accurate control relies on accurate positioning. Recently, the localization of autonomous vehicles based on the matching of Light Detection and Ranging (LiDAR) scan and High Definition (HD) map becomes the major solution. However, the matching can still possess meter-level positioning error in challenging areas with excessive dynamic vehicles or sparse features. Inaccurate positioning can result in obvious fluctuation in steering control of the vehicle subsequently, which is not acceptable for autonomous vehicles. In this paper, we propose to estimate the potential positioning uncertainty to further adaptively tune the parameters for the proportional-integral-derivative (PID) controller of vehicle steering. In this case, we can obtain a smoother control. Firstly, we generate the point cloud map of the tested area. Secondly, we correlate the uncertainty and optimal PID parameters using a fuzzy interference system. Finally, both the simulation and real experiments are conducted to validate the proposed method. The simulations show that the proposed adaptive PID controller is more resistant against unexpected positioning uncertainty and smoother control is obtained.

Keywords: Fuzzy Logic, Control, Localization, Positioning Uncertainty, Adaptive PID

I. INTRODUCTION

As artificial intelligence technology has a significant development in these several years, autonomous driving technology will be the way people traveled in the next decades-years [1]. Generally, the autonomous driving technique is subdivided into perception [9,10], localization [2,3,5], planning [36], and control [3,4] in academia and industry. Control is the lowest level of autonomous driving system. It receives information from all other modules which making it can be easily affected by the inaccurate output of the upper level especially localization. What will happen if the vehicle gives trusts to the incorrect localization result (the red dotted in the middle of Fig.1) given by the sensor while it is driving normally on the road? The vehicle will have suddenly harsh steering to keep on the 'right' lane, but it is a very dangerous action if there is a car coming towards us as shown in Figure 1.

This case may sometimes happen in real scenarios with inaccurate localization results, in this paper, we aim to optimize path tracking performance starting from the localization. To prove the proposed idea, we conducted several simulations and experiments in Hong Kong. For the localization part, a map-matching based method called normal distributions transform (NDT) matching is used. It matches the real-time scanned point cloud and pre-built HD map to localize vehicles. Biber and Strasser [11] first introduced NDT in which space is subdivided into 2D cells and in each cell. The environment is represented with normal distribution instead of the raw point cloud. Then Later Magnusson et al. extended the idea to the 3D domain [12,14]. For control, a number of novel methods [8,15,17] have been investigated in the previous studies including variant PID control methods [18,22,24-27,29,33,34] and Fuzzy control methods [19-21,23,28,30-32]. Although PID control is a simple, efficient, and widely used method,

* Manuscript received, July 26, 2020, final revision, December 2, 2020

** To whom correspondence should be addressed, E-mail: lt.hsu@polyu.edu.hk

it has limitations like controller parameters that cannot be changed dynamically. More studies combine PID with some novel artificial intelligence methods like fuzzy [31, 32] and [27, 33, 34] to improve classical PID. In this paper, a new Fuzzy-PID controller is designed to overcome the limitations of the traditional one. But due to the environment change and feature distribution of point cloud [13, 42], there may be a significant positioning error [37, 38, 39, 40], and this will cause an obvious control

fluctuation. Previous methods in literatures [18, 22, 40] make improvement from path planning and control, they did not correlate control and localization together. But if localization has a shift error, ego-vehicle trajectory tracking performance will not be satisfactory even if the controller is perfect. Thus, a new self-tuning Fuzzy PID controller considering localization error is proposed for lateral steering control to smooth the control fluctuations caused by NDT matching error.

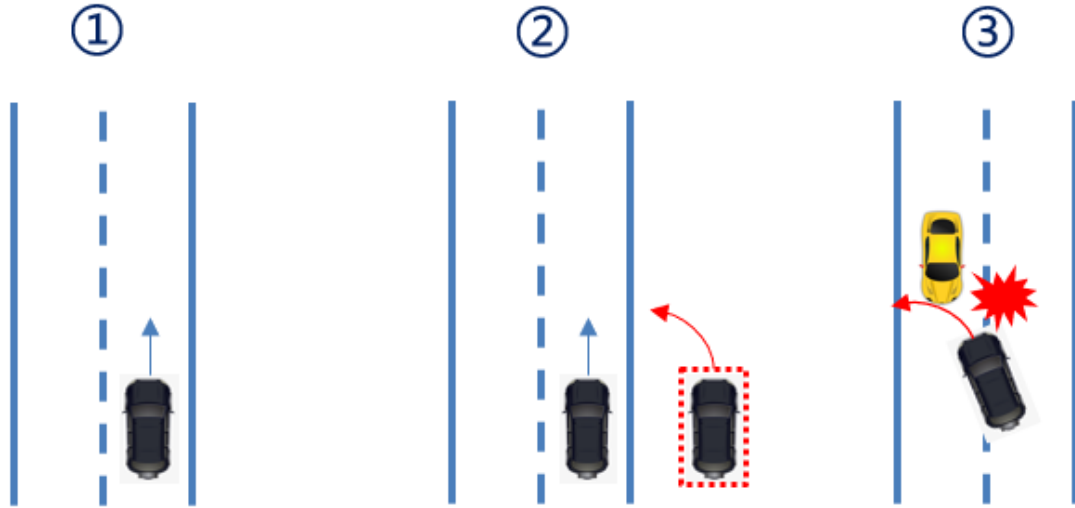


Figure 1 Localization jump may result in abnormal steering

The rest of the paper is organized as following: In the second chapter, the methods of the NDT-matching method and vehicle dynamic model are introduced. A closed-loop lateral steering control system is designed based on the vehicle dynamic model [16], and the Fuzzy PID controller is designed correlating positioning error and PID parameters. In the chapter three, experiments are conducted to collect LiDAR positioning data in the deep urban area of Hong Kong. Several simulations are conducted in Simulink to present the performance improvement of the new controller. Finally, the concluding remarks are given, and future work is suggested.

II. METHODS

2.1 NDT-Matching Localization

NDT-matching is a method for the localization of the vehicle on the map. The key to this algorithm is to register real-time scan point cloud data with a pre-built point cloud map. First, we should have an HD point cloud map and it can be built from simultaneous localization and mapping (SLAM) technique [35]. We subdivide the map into 3D cells as shown in Figure 2. In each cell, we model the distribution of points as the normal distribution. The NDT-matching method matches a LiDAR scan to the set of normal distribution rather than the raw point cloud.

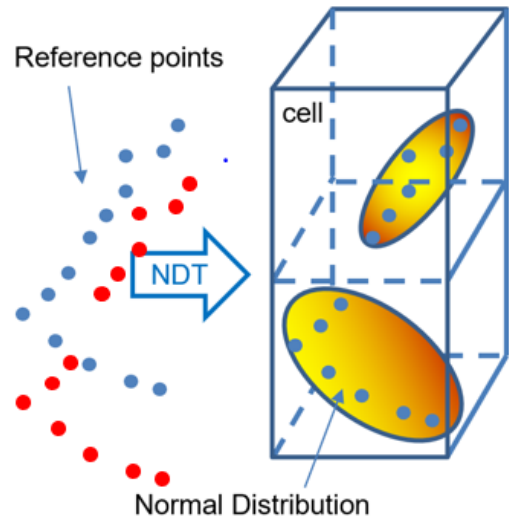


Figure 2 Point cloud distribution and matching between two sets of points

Then, the mean vectors and the covariance matrices are calculated in cells that contain at least five points. A probability that a point is located at position \mathbf{x} is calculated, it can be formulated as the probability density function as follows [11].

$$p(\mathbf{x}) = \frac{1}{c} \exp\left(-\frac{(\mathbf{x}-\boldsymbol{\mu})^T \boldsymbol{\Sigma}^{-1} (\mathbf{x}-\boldsymbol{\mu})}{2}\right) \quad (1)$$

where $\boldsymbol{\mu}$ and $\boldsymbol{\Sigma}$ denotes the mean vector and covariance matrix of the reference points in the cell which \mathbf{x} lies. Here the reference points mean the points in the pre-built HD map. \mathbf{x} is a vector representing the position in space of real-time scan points by LiDAR. For 3D space, \mathbf{x} is a vector as follows:

$$\mathbf{x} = \begin{bmatrix} x \\ y \\ z \end{bmatrix}$$

c is a normalizing constant that can be tuned heuristically. The mean and convenience matrix are computed as [11]:

$$\boldsymbol{\mu} = \frac{1}{m} \sum_{k=1}^m \mathbf{y}_k \quad (2)$$

$$\mathbf{T}(\mathbf{p}, \mathbf{x}) = \mathbf{R}\mathbf{x} + \mathbf{t} = \begin{bmatrix} c_y c_z & -c_y s_z & s_y \\ c_x s_z + s_x s_y s_z & c_x c_z - s_x s_y s_z & -s_x c_y \\ s_x s_z - c_x s_y c_z & c_x s_y s_z + s_x c_z & c_x c_y \end{bmatrix} \mathbf{x} + \begin{bmatrix} t_x \\ t_y \\ t_z \end{bmatrix} \quad (4)$$

where

\mathbf{R} is rotation matrix and \mathbf{t} is translation matrix, $c_i = \cos \phi_i$ and $s_i = \sin \phi_i$.

A set of points detected by LiDAR $\mathcal{X} = \{\mathbf{x}_1, \dots, \mathbf{x}_m\}$ are transformed by a pose \mathbf{p} and a transformation function $\mathbf{T}(\mathbf{p}, \mathbf{x})$. Then a probability score which is the sum of probability density function (PDF) of this set of points is defined:

$$s(p) = -\sum_{k=1}^m p(\mathbf{T}(\mathbf{p}, \mathbf{x})) \quad (5)$$

The purpose is to minimize this score function to get an optimized six-dimensional vector \mathbf{p} . In the algorithm, a \mathbf{p} is initialized. Then Newton's algorithm can be used to iteratively solve the equation $\mathbf{H}\Delta\mathbf{p} = -\mathbf{g}$, where \mathbf{H} and \mathbf{g} are the Hessian and gradient of s . The increment $\Delta\mathbf{p}$ is added to the current estimate of the parameter in each iteration so that $\mathbf{p} \leftarrow \mathbf{p} + \Delta\mathbf{p}$. Once \mathbf{p} is found, the position in the map can be obtained.

2.2 Vehicle lateral controller design

The lateral controller design is based on the vehicle dynamic model. We consider the four-wheel vehicle as a two-degree bicycle model. The two degrees of freedom are vehicle lateral position y and vehicle yaw angle ψ . The lateral position is defined from the center of gravity to the lateral axis of the vehicle. The vehicle yaw angle is measured in the local frame concerning X-axis and the longitudinal velocity V_x is measured at the center of gravity. Vehicle mass is m .

Figure 3 shows the lateral motion of the vehicle dynamic model in local frame XY, body frame XY is fixed on the center of the vehicle. ψ and ψ_{des} denote current heading angle and desired to head angle respectively. According to Newton's second law, the motion along y-axis can be described as:

$$ma_y = F_{yf} + F_{yr} \quad (6)$$

where a_y is the inertial acceleration of the vehicle at the center of gravity of y-axis and F_{yf} and F_{yr} are the lateral tire forces of front and rear wheels respectively. a_y

$$\boldsymbol{\Sigma} = \frac{1}{m-1} \sum_{k=1}^m (\mathbf{y}_k - \boldsymbol{\mu})(\mathbf{y}_k - \boldsymbol{\mu})^T \quad (3)$$

where $\mathbf{y}_{k=1, \dots, m}$ are the position of reference scan points contained in the cell.

After we model the environment by a normal distribution, we register the scan. The purpose is to find the pose of the current scan that maximizes the likelihood that the points of the current scan lie on the reference scan. We encode the translation and rotation of estimates current pose as a six-dimensional vector $\mathbf{p} = [t_x, t_y, t_z, \phi_x, \phi_y, \phi_z]^T$. Using the Euler sequence z-y-x, the 3D transformation function is [12]:

can be written as Equation 8. \ddot{y} is acceleration along y-axis and $V_x \dot{\psi}$ is the centripetal acceleration.

$$a_y = \ddot{y} + V_x \dot{\psi} \quad (7)$$

Substitute Equation 7 into 6, the equation can be written as:

$$m(\ddot{y} + \dot{\psi} V_x) = F_{yf} + F_{yr} \quad (8)$$

and the moment balance on the z-axis is:

$$I_z \ddot{\psi} = l_f F_{yf} - l_r F_{yr} \quad (9)$$

where I_z is the moment of inertia about z-axis and $\ddot{\psi}$ is angular acceleration. Equation 8 and 9 are the two fundamental equations representing the lateral motion of the vehicle.

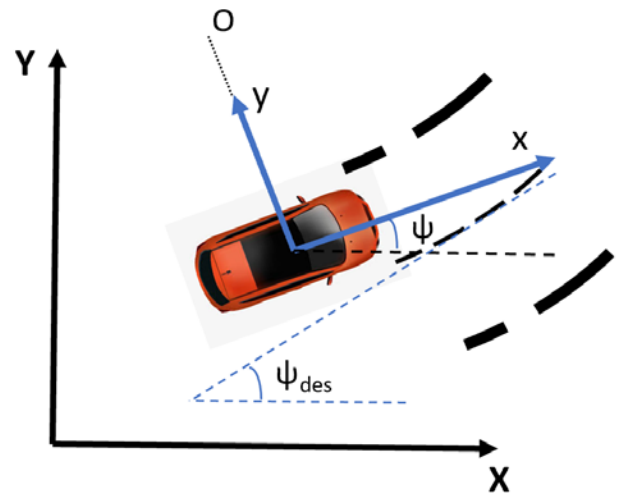


Figure 3 Lateral motion of the vehicle dynamic model described by the two-degree bicycle model

Generally, the force is proportional to the slip-angle for a small slip-angle. But when slip-angle gets larger, the relationship becomes nonlinear. The slip angle of the front and the rear wheel is:

$$\alpha_f = \delta - \theta_{Vf} \quad (10)$$

$$\alpha_r = -\theta_{Vr} \quad (11)$$

where θ_{Vf} and θ_{Vr} are the angle between the velocity vector and vehicle longitudinal direction in Figure 4. δ is the front wheel angle.

The lateral force for both can be described as:

$$F_{yf} = 2C_{\alpha f}(\delta - \theta_{Vf}) \quad (12)$$

$$F_{yr} = 2C_{\alpha r}(-\theta_{Vr}) \quad (13)$$

where the constant $C_{\alpha f}$ and $C_{\alpha r}$ are called cornering stiffness of front and rear tires. The constant 2 means there are two front wheels and rear wheels. The unknown factors are θ_{Vf} and θ_{Vr} . Assuming we have a relationship [16]:

$$\tan(\theta_{Vf}) = \frac{v_y + l_f \dot{\psi}}{v_x} \quad (14)$$

$$\tan(\theta_{Vr}) = \frac{v_y - l_r \dot{\psi}}{v_x} \quad (15)$$



Figure 4 Description of tire slip angle in the two-degree bicycle model

If we use small approximations and using the notation $V_y = \dot{y}$, we have

$$\theta_{Vf} = \frac{\dot{y} + l_f \dot{\psi}}{v_x} \quad (16)$$

$$\theta_{Vr} = \frac{\dot{y} - l_r \dot{\psi}}{v_x} \quad (17)$$

So far the Equation 8 and 9 of lateral vehicle dynamics can be represented by state-space model as $\dot{\mathbf{X}} = \mathbf{A}\mathbf{X} + \mathbf{B}\mathbf{U}$ as Equation 18.

$$\frac{d}{dt} \begin{Bmatrix} y \\ \dot{y} \\ \psi \\ \dot{\psi} \end{Bmatrix} = \begin{bmatrix} 0 & 1 & 0 & 0 \\ 0 & -\frac{2C_{\alpha f} + 2C_{\alpha r}}{m v_x} & 0 & -V_x - \frac{2l_f C_{\alpha f} - 2l_r C_{\alpha r}}{m v_x} \\ 0 & 0 & 0 & 1 \\ 0 & -\frac{2l_f C_{\alpha f} - 2l_r C_{\alpha r}}{v_x I_z} & 0 & -\frac{2l_f^2 C_{\alpha f} + 2l_r^2 C_{\alpha r}}{v_x I_z} \end{bmatrix} \begin{Bmatrix} y \\ \dot{y} \\ \psi \\ \dot{\psi} \end{Bmatrix} + \begin{Bmatrix} 0 \\ \frac{2C_{\alpha f}}{m} \\ 0 \\ \frac{2l_f C_{\alpha f}}{I_z} \end{Bmatrix} \delta \quad (18)$$

column vector $[y \ \dot{y} \ \psi \ \dot{\psi}]$ is a state vector in which y is lateral position and ψ is heading angle, δ is input as wheel angle. The 4-by-4 matrix here is the dynamics matrix in which $C_{\alpha f}$ and $C_{\alpha r}$ are cornering stiffness, I_z is the moment of inertia, V_x is longitudinal velocity, l_f and l_r are the distance from the front wheel and rear wheel to the center of gravity respectively, m is mass. 4-by-1 matrix is the input matrix here.

Based on the derivation mentioned above, the system is designed in Simulink as shown in Figure 5. The vehicle dynamic module is designed based on the model

described in Equation (18), the velocity and steering are fed into it and outputs yaw rate, longitudinal velocity, and lateral velocity to the next module. The steering controller combines that upstream information with a given specific road curvature to calculate steering error, which is the offset between ego-car's heading and desired heading related to the road. Then the key to the system is the Fuzzy PID, which calculates a steering output given a steering error with the controller parameter determined by probability score and its change rate of localization module.

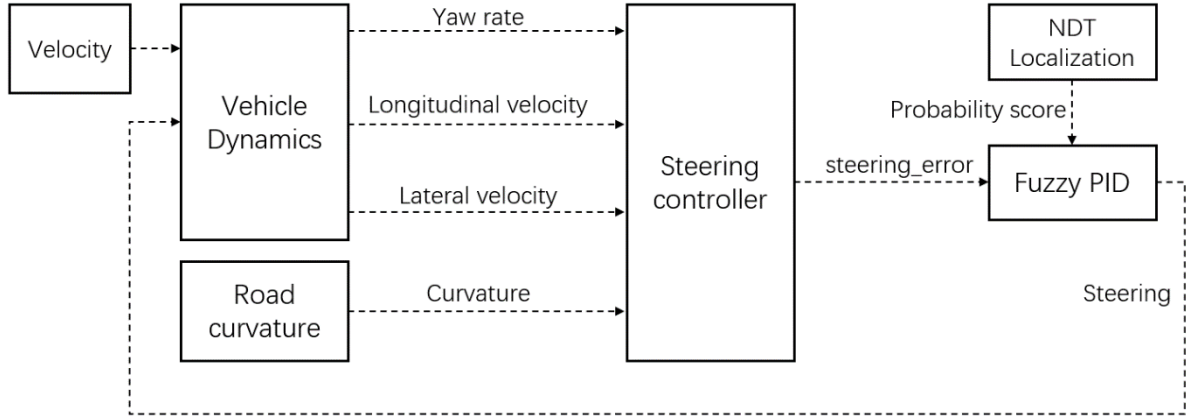


Figure 5 Design of the proposed lateral control system to mitigate the effect of the NDT localization uncertainty.

The steering controller calculates a combined steering error which is the sum of heading offset and lateral displacement offset of ego-car related to current road curvature, equations are shown in Equation 19 and 20.

$$\dot{e}_1 = V_x e_2 + V_y \quad (19)$$

$$e_2 = \psi - \psi_{des} \quad (20)$$

ψ_{des} is the desired yaw rate given by $\frac{V_x}{R}$ which R is the radius for the road curvature. e_1 and e_2 are lateral displacement error and yaw angle error, respectively.

In the Fuzzy PID module, there are two submodules; One is the Fuzzy Logic module correlating NDT localization and PID controller, another one is a classical PID closed-loop control system. The control function in the time domain could be expressed mathematically as:

$$u(t) = K_p e + K_d \frac{de}{dt} \quad (21)$$

where K_p , K_d contribute the proportional, and derivative terms respectively. e is the combined steering error and u is the control variable which is wheel steering. Some parameters of vehicle dynamics are shown in Table 1.

Table1 Vehicle dynamic parameters used in this paper.

Vehicle parameter	Value
vehicle mass (kg)	1575
vehicle yaw moment inertia (kg*m ²)	2875
longitudinal distance from the center of mass to the front axle (m)	1.2
longitudinal distance from the center of mass to rear axle (m)	1.6
front tire corner stiffness Cf (N/rad)	19000
rear tire corner stiffness Cr (N/rad)	33000

2.3 Fuzzy system design

The Fuzzy PID controller is designed to tune controller parameters adaptively and its architecture is shown in Figure 6. Probability score s of NDT-matching

calculated in Equation 6 and its change rate $\frac{dP}{dt}$ are set as inputs of fuzzy system, K_p and K_d are set as outputs of it.

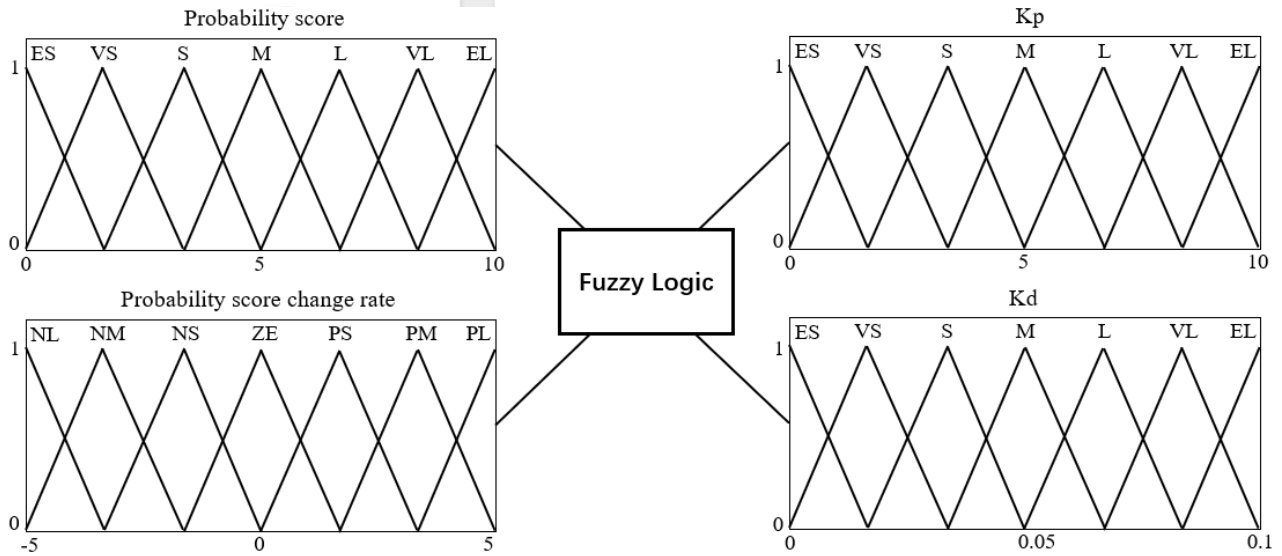


Figure 6 Architecture of the proposed fuzzy logic: 2 inputs and 2 outputs

The range of probability score of 2.0m grid size is $[0, 10]$ and the range of probability score change rate is $[-5, 5]$. In our simulation, the range of K_p , K_d are decided as $[0, 10]$ and $[0, 0.1]$ respectively and if they are out of this range, the system will be unstable. For each

input and output, 7 triangular membership functions are used to describe them mathematically. The meaning of linguistic variables of the membership function is shown in Table 2.

Table 2 Definition of the membership functions of fuzzy system

Membership function	Abbreviated	Membership function	Abbreviated
Extremely Small	ES	Negative Large	NL
Very Small	VS	Negative Medium	NM
Small	S	Negative Small	NS
Medium	M	Zero	ZE
Large	L	Positively Small	PS
Very Large	VL	Positively Medium	PM
Extremely Large	EL	Positively Large	PL

The main process of fuzzy rules design is shown as Figure 7. Once NDT localization has a jump, the probability score P calculated in Equation (5) will become a smaller value and its change rate dP will get larger normally as P changes. Via fuzzy rules, we want to decrease K_p value because we want to minimize

proportional response of steering output. And we also want to increase K_d value to increase dampening effect of rapid change. After K_p and K_d change, control output steering wheel angle will get smaller so that we can smooth lateral tracking error.

III. EXPERIMENT RESULTS AND DISCUSSIONS

3.1 Experiment

To simulate the Fuzzy controller in Simulink and evaluate its performance, an experiment was conducted in Whampoa, a dense urban area of Hong Kong. Data is

collected by our data collection platform and sensor kit is mounted on the top of the car like shown in Figure 8. The point cloud data is collected by Velodyne 32E LiDAR and ground truth of trajectory is provided by Novatel SPAN-CPT, which is dual-frequency GNSS RTK integrated with fiber optics gyroscope.



Figure 8 Data collection platform and sensors: including Fisheye camera, Velodyne 32E LiDAR, IMU and Novatel SPAN-CPT

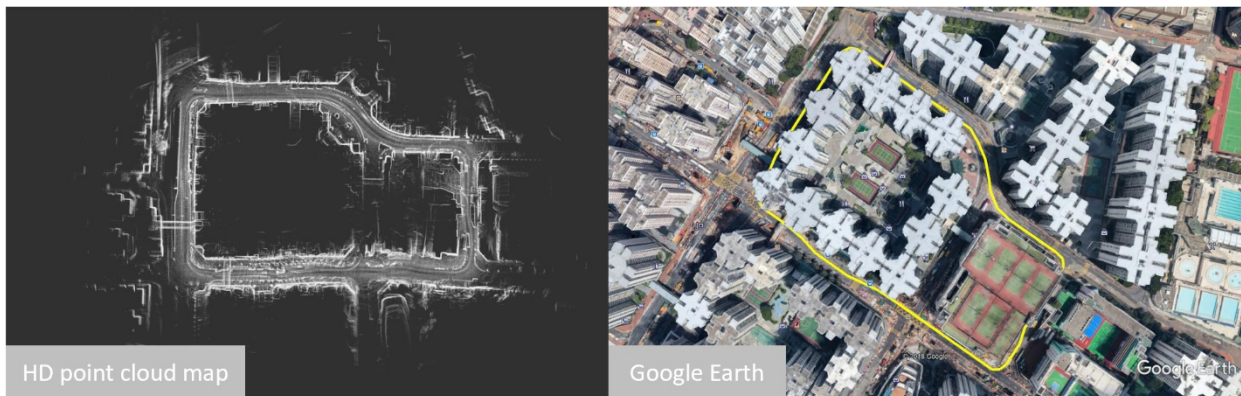


Figure 9 (Left) Experiment area (Right) HD map generated by the LiDAR SLAM.

The point cloud map made by Velodyne 32E LiDAR and the experiment area from Google Earth can be seen in Figure 9. After collecting the data, the self-localization is performed based on NDT-matching with a 2m grid size. The process of NDT-matching is demonstrated in Figure 10. Then the localization error of NDT-matching is obtained by comparing it with the positioning results of

SPAN-CPT. The probability score of NDT-matching calculated in Equation (5) is also obtained. Their correlation is shown in Figure 11. The probability score and positioning error have a negative correlation of -0.83 correlation coefficient. The two biggest errors appear in around 80 seconds and 200 seconds.

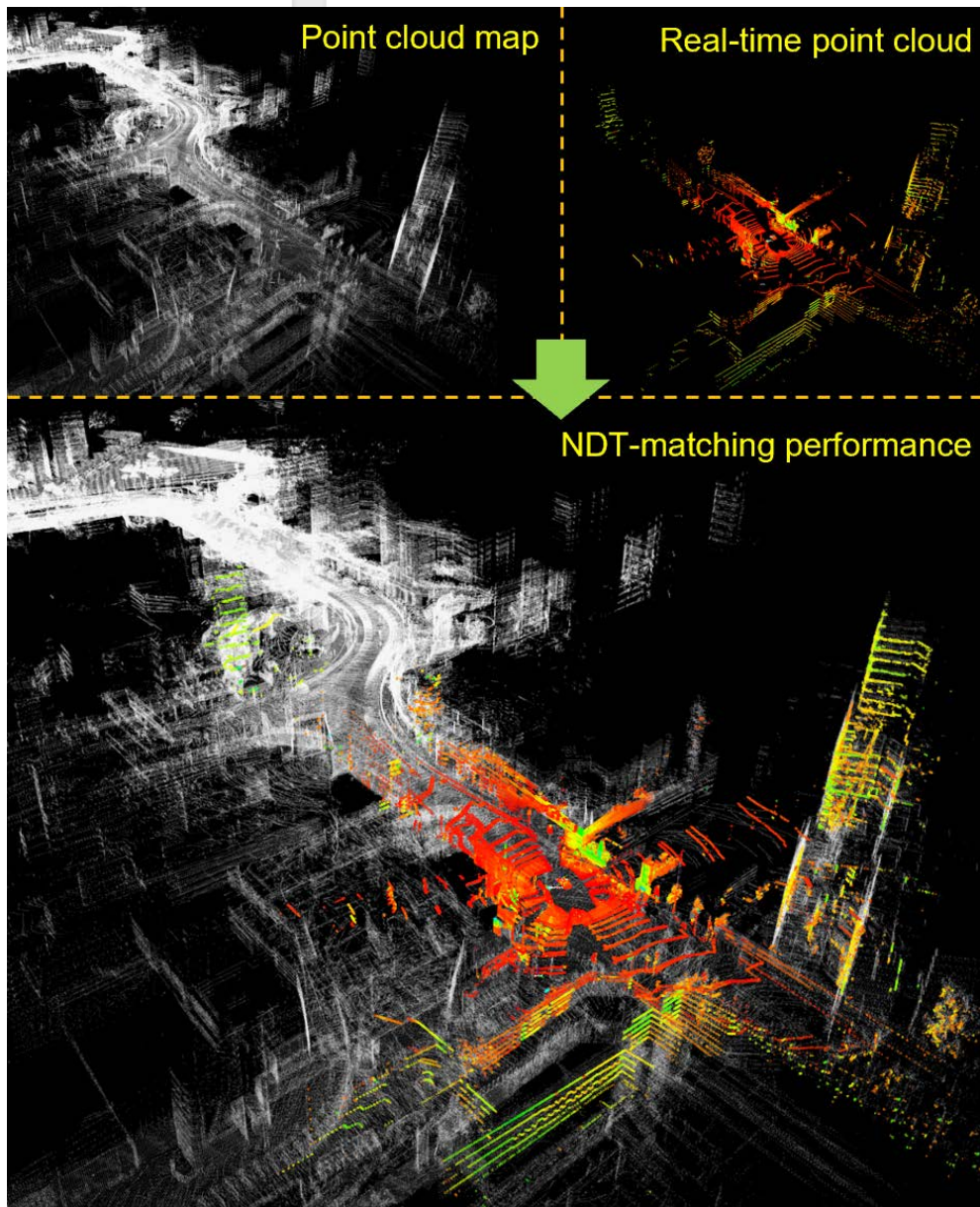


Figure 10. NDT-matching process

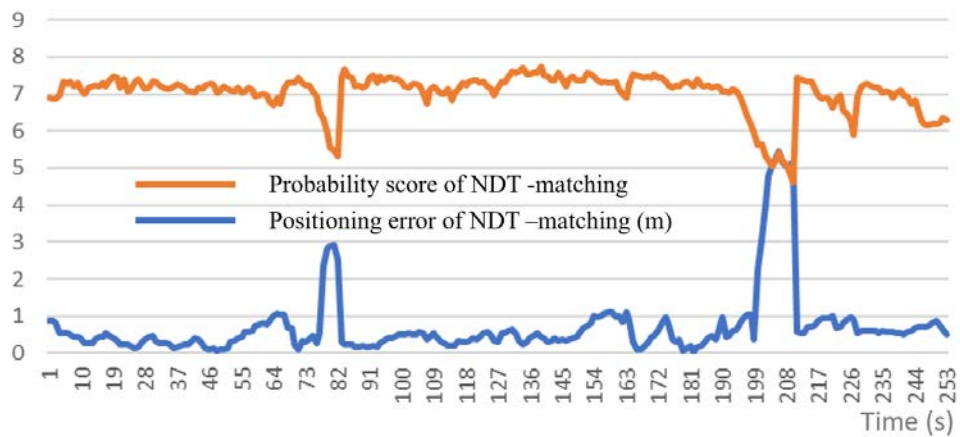


Figure 11 NDT-matching localization error and probability score of the LiDAR matching

3.2 Simulation

In this section, three simulations are conducted in Simulink to verify the performance of new design controller. We simulate ego car is driving on a smooth road of free limit area with 1/750 curvature, and for safety reason the longitudinal velocity is set as 1m/s. In the first simulation, the initial position of the vehicle is (0,0) in the

local frame and the initial yaw angle is 0 radius. The K_p and K_d of the PID controller are set as 10 and 0.1 theoretically and experimentally so that ego car can drive a smooth trajectory without oscillation. The trajectory is shown in Fig 12 during simulation time of 252 seconds, it will be used as a reference in the following simulations.

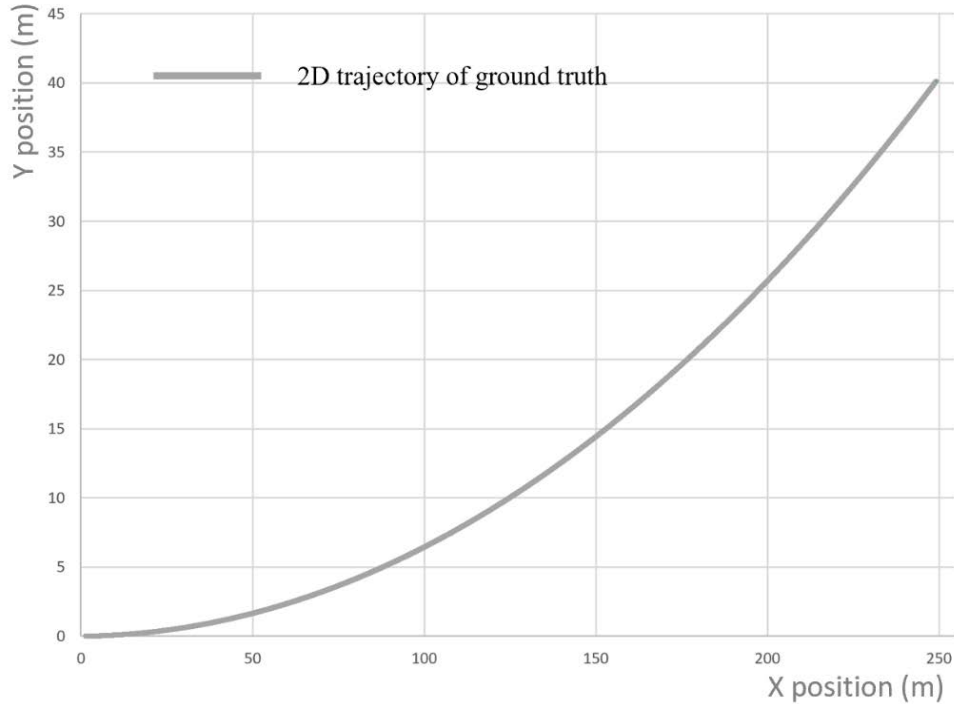


Figure 12 2D trajectory of convention PID controller

Above simulation is under perfect condition. But in real scenario, there are errors introduced by the external environment. The errors consist of two sources; one is control error; one is sensor error. Control error comes from the imperfect modelling due to the changes of road surface and vehicle hardware. Sensor error comes from the positioning error of sensors. To simulate sensor error, the NDT matching positioning error of the experiment is introduced into a simulation system manually. The second simulation results after introducing NDT-matching error is shown in Figure 13, it has a fluctuation since positioning error influences control stability, especially at around 80s and 200s. These two huge errors eventually cause an offset

of the trajectory. We can see that the vehicle almost has a U-turn in the 80s because of the “wrong” control commands and the offset of trajectory increases about 5m from 200s. It is dangerous when a driverless car is driving like this, it may bring damage to the traffic and people.

To smooth big errors, the third simulation using Fuzzy PID controller which designed in section 2.3 is conducted in the same scenario. Trajectory result is shown in Figure 14, the blue line represents conventional PID controller and the orange line represents the Fuzzy PID controller. We can see that Fuzzy controller corrects the trajectory at 80s and 200s, it is smoother than the conventional one. It can mostly follow the ground truth.

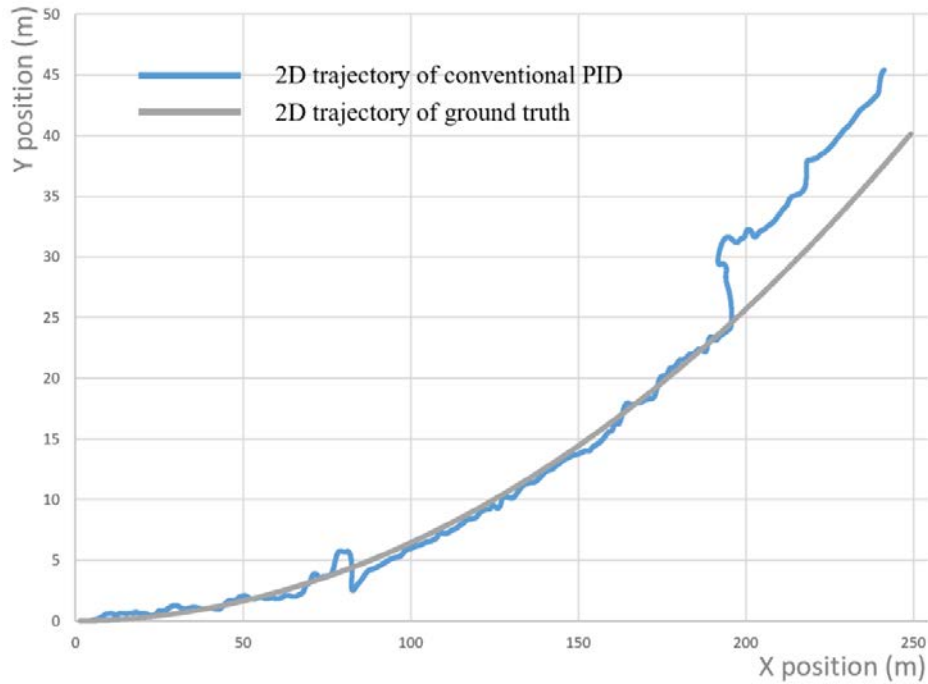


Figure 13 The 2D trajectory of convention PID controller and ground truth after introducing NDT-matching error

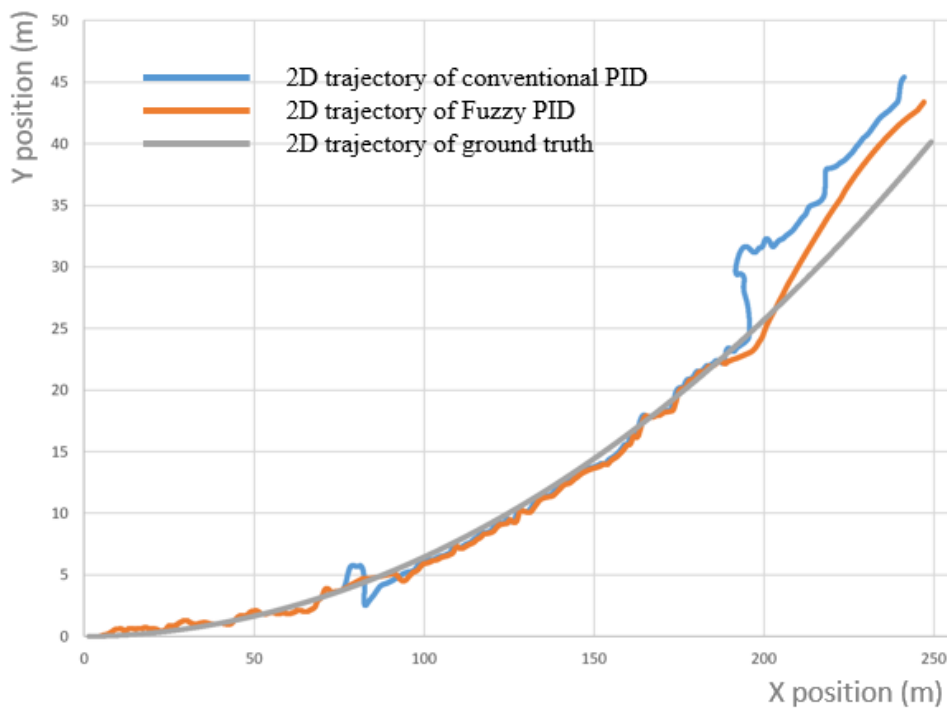


Figure 14 The 2D trajectory of conventional PID controller, Fuzzy PID controller and ground truth changing with simulation time

Figure 15 compares the correlation between different variables in the simulation including lateral displacement error, probability score, and its change rate, K_p and K_d , steering angle, and yaw angle. In the A-B and C-D periods, localization shows high accuracy. However, in B-C and E-F high error appeared. These errors come from low probability score and high probability score

change rate which can be seen from the second and third lines. K_p and K_d are highly related to the probability score, they have a significant decrease during period B-C and E-F. The steering angle and yaw angle of the conventional PID controller and Fuzzy PID controller are almost the same during period A-B and C-E, but they significantly decrease within B-C and E-F.

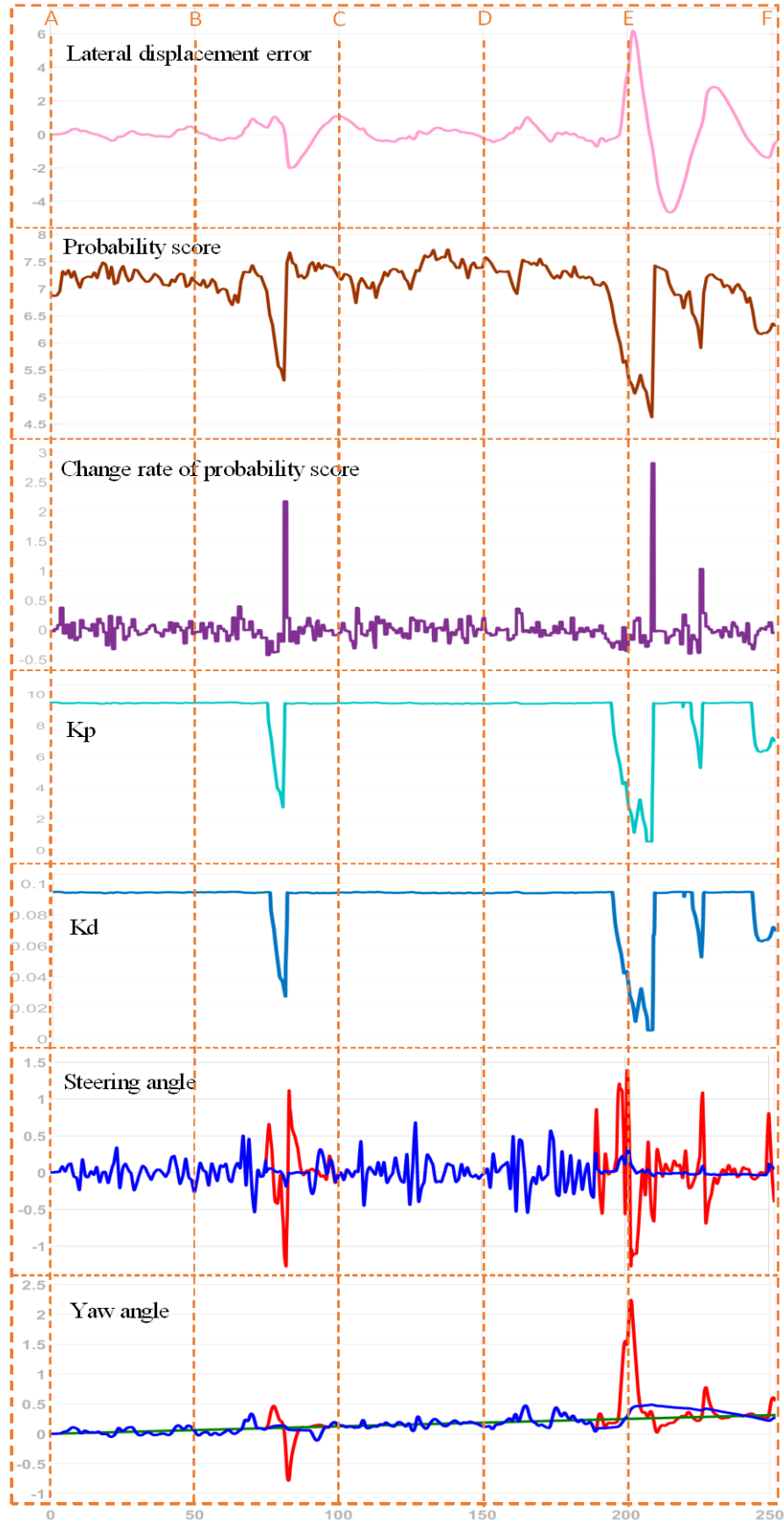


Figure 15 Correlation between the LiDAR NDT error, probability score, K_p , K_d and the controlled steering angle and resulted yaw angle.

First block of figure 16 denotes how the Fuzzy controller improves trajectory tracking performance. Top three lines represent X position in the local frame and three lines at the bottom represent Y position in the local frame. Zoom in four orange areas 1-4, we can see that the conventional controller has approximately 0.5m error for

both X and Y position at the time around the 80s, however, the fuzzy controller has almost the same results as ground truth. At the time of 200s, the convention controller has about 1m error, but the fuzzy controller has a much better result. The controller has better performance on the X position than Y.

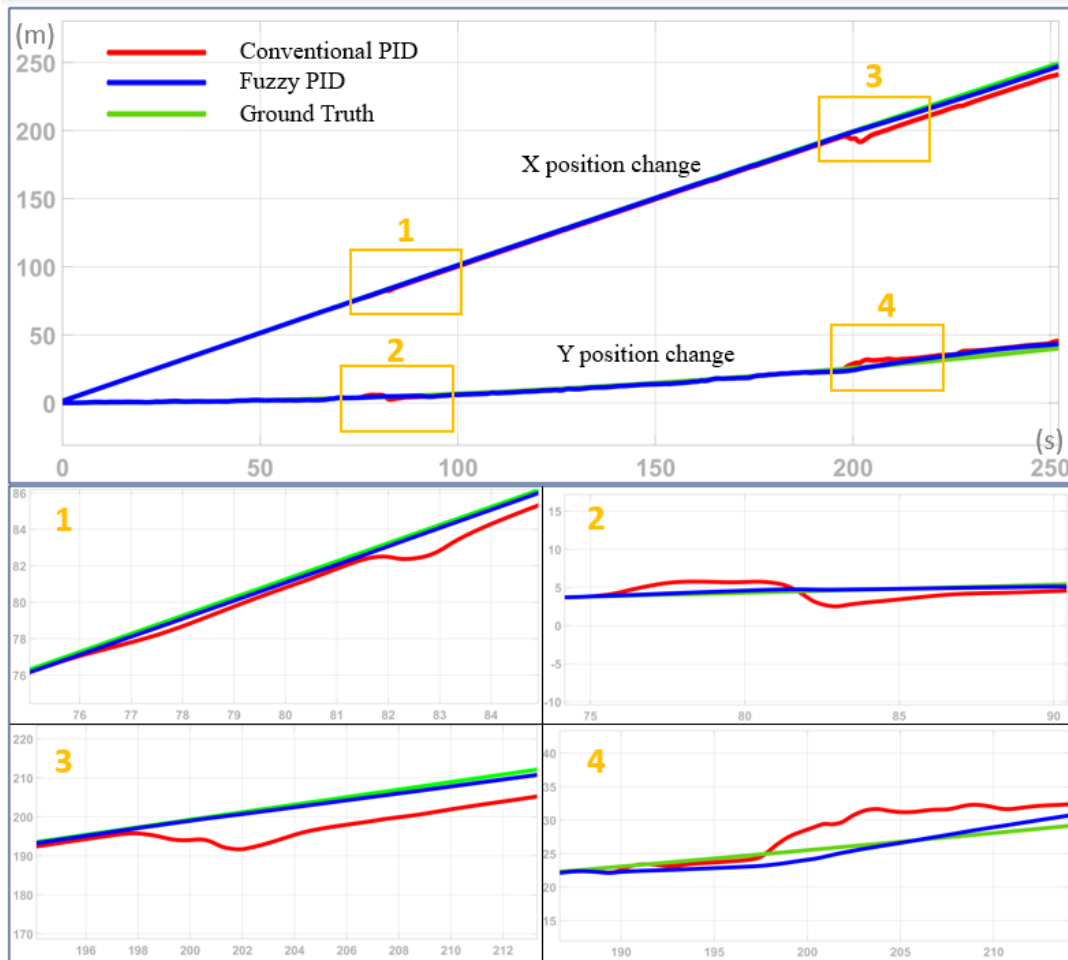


Figure 16 X and Y position change of conventional PID controller, Fuzzy PID controller and ground truth changing with simulation time

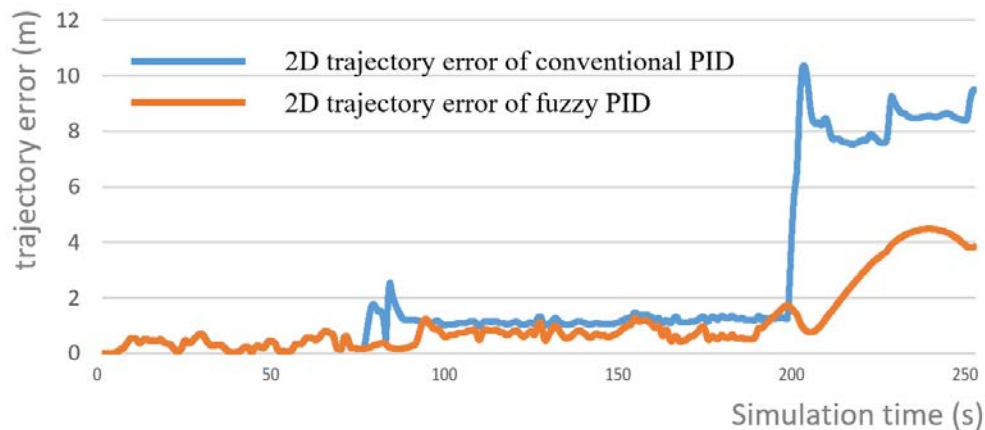


Figure 17 The 2D Trajectory error of a conventional PID controller and Fuzzy PID controller changing with simulation time

Table 5 Trajectory tracking performance of the conventional PID controller and Fuzzy PID controller

Controller \ Error	Mean (m)	Std (m)	Max (m)
Conventional PID	2.42	3.07	10.38
Fuzzy PID	1.09	1.22	4.48

Figure 21 shows the 2D trajectory of three different controllers. We can see that the vehicle trajectory of the fuzzy controller is not affected seriously by positioning error in the 80s. It does not make U-turn like a conventional controller and smooth the error well. After 200s, although the trajectory has offset with the desired one, it still has improvement and smoother. The trajectory error of two controllers is compared numerically in Figure 22 and Table 4. They are the same values before the 80s, and it has a significant decrease after the 80s especially after the 200s. The fuzzy controller reduces mean error and standard deviation of trajectory error from 2.42m to 1m and from 3.07m to 1.22m respectively.

IV. CONCLUSIONS AND FUTURE WORK

In this work, we focused on the correlation between localization and lateral control of the autonomous vehicles. For localization, the NDT-matching method is performed to localize the vehicle's position by aligning real-time point cloud with point cloud map. We use the probability score to predict NDT-matching positioning error. Then the vehicle dynamic model is introduced, and we design a PID lateral controller based on it. The controller adjusts the steering angle of the front wheel to follow the desired trajectory. But in challenging scenarios, erroneous positioning can eventually result in steering fluctuations. To smooth these fluctuations, a fuzzy PID controller is designed, it adaptively adjusts the PD gain parameters based on the probability score and its change rate of NDT-matching.

we collected point cloud data from LiDAR in an urban area at Hong Kong, and the point cloud map is generated. Then NDT-matching method is performed to obtain positioning error by comparing them with SPAN-CPT. We have found that NDT-matching positioning error has a high correlation with its probability score.

To evaluate the performance of the proposed fuzzy PID controller, several simulations have conducted in Simulink. The vehicle follows the same path with fuzzy PID controller, it has a significant improvement. The mean error of trajectory tracking has been decreased by more than 1 meter and the maximum error reduces from 10 meters to 4 meters.

However, the presented method still has some drawback: 1) Sometimes the correlation between

probability score and localization error is weak; 2) the fuzzy rules are simple that may cannot cover all cases. 3) the accuracy of lateral control using PID is limited. In the future, we will find other factors correlating well with localization error in different scenarios and optimize fuzzy rules. Apart from this, we will apply this method on more different controller to solve control instability.

Biographies

Hu Sai is a M.Sc. graduate at the Department of Mechanical Engineering, the Hong Kong Polytechnic University, Hong Kong. His research area includes control, vehicle dynamics and LiDAR localization of autonomous vehicles.

Li-Ta Hsu received the B.S. and Ph.D. degrees in aeronautics and astronautics from National Cheng Kung University, Taiwan, in 2007 and 2013, respectively. He is currently an assistant professor with the Interdisciplinary Division of Aeronautical and Aviation Engineering, The Hong Kong Polytechnic University, before he served as a post-doctoral researcher in the Institute of Industrial Science at the University of Tokyo, Japan. In 2012, he was a visiting scholar in University College London, the U.K. His research interests include GNSS positioning in challenging environments and localization for pedestrian, autonomous driving vehicle and unmanned aerial vehicle.

REFERENCES

- [1] Montemerlo M, Becker J, Bhat S, Dahlkamp H, Dolgov D, Ettinger S, Haehnel D, et al., "Junior: The Stanford Entry in the Urban Challenge," *Journal of Field Robotics*, Vol. 25, No. 9, 2008, pp. 569–597.
- [2] Levinson J, Montemerlo M, Thrun S, "Map-Based Precision Vehicle Localization in Urban Environments," in *Robotics Science and Systems*, 2007.
- [3] Nejad HTN, Do QH, Sakai R, Han L, "Real time localization, path planning and motion control for autonomous parking in cluttered environment with narrow passages," In *Proceedings of the International IEEE Conference on Intelligent Transportation Systems*, Anchorage, AK, USA, 16–19 September 2012; pp. 1357–1364.
- [4] Tagne G, Talj R, Charara A, "Higher-order sliding mode control for lateral dynamics of autonomous vehicles, with experimental validation," In *Proceedings of the Intelligent Vehicles Symposium*, Gold Coast, QLD, Australia, 23–26 June 2013; pp. 678–683.
- [5] Takezawa S, Gulrez T, Herath DC, Dissanayake G, "Environmental Recognition for Autonomous Robot using Simultaneous Localization and Map Building (SLAM) (Real Time Path Planning with Dynamical Localized Voronoi Division)," *Transactions of the Japan Society of Mechanical Engineers*, Vol. 71, 2005, pp. 904–911.
- [6] Wang X, Fu M, Yang Y, Ma H, "Lateral Control of Autonomous Vehicles Based on Fuzzy Logic," In

- Proceedings of the Control and Decision Conference, Guiyang, China, 25–27 May 2013; pp. 237–242.
- [7] Tagne G, Talj R., Charara A, “Design and validation of a robust immersion and invariance controller for the lateral dynamics of intelligent vehicles,” *Control Engineering Practice*. Vol. 40, 2015, pp. 81–92.
- [8] You F, Wang RB, Zhang RH, “Study of System Identification and Control Algorithm for Intelligent Vehicle,” *China Journal of Highway and Transport*, Vol. 125, 2008, pp. 749–752.
- [9] Teichman A, Levinson J, Thrun S, “Towards 3D Object Recognition via Classification of Arbitrary Object Tracks,” in International Conference on Robotics and Automation, 2011.
- [10] Levinson J, Askeland J, Becker J, Dolson J, Held D, Kammel S, Kolter JZ, Langer D, Pink O, Pratt VR, Sokolsky M, Stanek G, Stavens D, Teichman A, Werling M, Thrun S, “Towards fully autonomous driving: Systems and algorithms,” 2011 IEEE Intelligent Vehicles Symposium (IV), pp. 163-168.
- [11] Biber P, Strasser W, “The normal distributions transform: A new approach to laser scan matching,” in Proceedings IEEE/RSJ International Conference on Intelligent Robots and Systems (IROS), Vol. 3, Oct. 2003, pp. 2743-2748.
- [12] Magnusson M, Lilienthal A, Duckett T, “Scan registration for autonomous mining vehicles using 3D-NDT,” *Journal of Field Robotics*, Vol. 24, No. 10, 2007, pp. 803-827.
- [13] Javanmardi E, Javanmardi M, Gu Y, Kamijo S, “Factors to Evaluate Capability of Map for Vehicle Localization,” *IEEE Access*, Vol. 6, 2018, pp. 49850-49867.
- [14] Akai N, Morales LY, Takeuchi E, Yoshihara Y, Ninomiya Y, “Robust localization using 3D NDT scan matching with experimentally determined uncertainty and road marker matching,” 2017 IEEE Intelligent Vehicles Symposium (IV), Los Angeles, CA, 2017, pp. 1356-1363, doi: 10.1109/IVS.2017.7995900.
- [15] Man HL, Park HG, Lee SH, Kang SY, Lee KS, “An adaptive cruise control system for autonomous vehicles,” *International Journal of Precision Engineering and Manufacturing*, Vol. 14, 2013, pp. 373–380.
- [16] Rajamani R, 2006, *Vehicle Dynamics and Control*, 10.1007/0-387-28823-6.
- [17] Netto MS, Chaib S, Mammari S, “Lateral adaptive control for vehicle lane keeping,” In Proceedings of the American Control Conference, Boston, MA, USA, 30 June–2 July 2004; Vol. 2693, pp. 2693–2698.
- [18] Zhao P, Chen J, Song Y, Tao X, Xu T, Mei T, “Design of a Control System for an Autonomous Vehicle Based on Adaptive-PID,” *International Journal of Advanced Robotic Systems*, 2012.
- [19] Yang Y, Yang W, Wu M, Yang Q, Xue Y, “A new type of adaptive fuzzy PID controller,” 2010 8th World Congress on Intelligent Control and Automation, Jinan, 2010, pp. 5306-5310, doi: 10.1109/WCICA.2010.5554827.
- [20] Khodayari MH, Balochian S, “Modeling and control of autonomous underwater vehicle (AUV) in heading and depth attitude via self-adaptive fuzzy PID controller,” *Journal of Marine Science and Technology*, Vol. 20, 2015, pp. 559–578, <https://doi.org/10.1007/s00773-015-0312-7>.
- [21] Xu J, Feng X, “Design of adaptive fuzzy PID tuner using optimization method,” Fifth World Congress on Intelligent Control and Automation (IEEE Cat. No.04EX788), Hangzhou, China, Vol. 3, 2004, pp. 2454-2458, doi: 10.1109/WCICA.2004.1342035.
- [22] Han G, Fu W, Wang W, Wu Z, “The Lateral Tracking Control for the Intelligent Vehicle Based on Adaptive PID Neural Network,” *Sensors*. Vol. 17, 2017, pp. 1244. 10.3390/s17061244.
- [23] Tang KS, Man KF, Chen G, Kwong S, “An optimal fuzzy PID controller,” *IEEE Transactions on Industrial Electronics*, Vol. 48, No. 4, 2001, pp. 757-765, doi: 10.1109/41.937407.
- [24] Jiao J, Chen WW, Li SW, Wang JX, “Self-adaptive PID control for intelligent vehicle steering system based on IPSO,” *Journal of Anhui University*, Vol. 29, 2008, pp. 1325–1327.
- [25] Yamamoto T, Takao K, “Design and Experimental Evaluation of a Data-Driven PID Controller,” *IFAC Proceedings Volumes*, Vol. 40, 2010, pp. 391–396.
- [26] Marino R, Scalzi S, Orlando G, Netto M, “A Nested PID Steering Control for Lane Keeping in Vision Based Autonomous Vehicles,” *Proceedings of the American Control Conference*, 2009, pp. 2885 - 2890. 10.1109/ACC.2009.5160343.
- [27] Rodrigo HA, Govinda GVL, Tomás SJ, Alfonso, GE, Fernando FN, “Neural Network-Based Self-Tuning PID Control for Underwater Vehicles,” *Sensors*, Vol. 16, 2016, pp. 1429.
- [28] Economou JT, Colyer RE, Tsourdos A, White BA., “Fuzzy logic approaches for wheeled skid-steer vehicles,” In Proceedings of the 2002 IEEE Vehicular Technology Conference, Vancouver, BC, Canada, 24–28 September 2002; Volume 992, pp. 990–994.
- [29] Rout R, Subudhi B, “Inverse optimal self-tuning PID control design for an autonomous underwater vehicle,” *International Journal of Systems Science*, Vol. 48, 2016, pp. 367–375.
- [30] Naranjo JE, González C, García R, Pedro TD, “Lane-Change Fuzzy Control in Autonomous Vehicles for the Overtaking Maneuver,” *IEEE Transactions on Intelligent Transportation Systems*, Vol. 9, 2008, pp. 438-450.
- [31] Cai L, Rad AB, Chan WL, Cai, KY, “A robust fuzzy PID controller for automatic steering control of autonomous vehicles,” *IEEE International Conference on Fuzzy Systems*, Vol. 1, 2003, pp. 549 – 554, 10.1109/FUZZ.2003.1209423.
- [32] Dong HF, Li F, Gao QJ, Dong BL, “Research on Intelligent Vehicle Steering System via Improved

- Fuzzy-PID Control Method Based on RSDA,” *Applied Mechanics and Materials*, Vol. 220-223, 2012, pp. 958-963.
- [33] Zhenhai G, Bo Z, “Vehicle lane keeping of adaptive PID control with BP neural network self-tuning,” In *Proceedings of the Intelligent Vehicles Symposium*, Las Vegas, NV, USA, 6-8 June 2005; pp. 84-87.
- [34] Zhang GD, Yang XH, Lu DQ, Liu YX, “Research on Pressurizer Pressure Control System Based on BP Neural Network Control of Self-Adjusted PID Parameters,” *Applied Mechanics and Materials*, Vol. 294, 2013, pp. 2416-2423.
- [35] Kato S, et al., “Autoware on Board: Enabling Autonomous Vehicles with Embedded Systems,” 2018 ACM/IEEE 9th International Conference on Cyber-Physical Systems (ICCPS), Porto, 2018, pp. 287-296, doi: 10.1109/ICCPS.2018.00035.
- [36] Zhang GH, Hsu LT, (2018), “Intelligent GNSS/INS integrated navigation system for a commercial UAV flight control system,” *Aerospace Science and Technology*. 80. 10.1016/j.ast.2018.07.026.
- [37] Wen W, Bai X, Zhan W, Tomizuka M, Hsu LT, (2019), “Uncertainty Estimation of LiDAR Matching Aided by Dynamic Vehicle Detection and High Definition Map,” *Electronics Letters*. 55. 10.1049/el.2018.8075.
- [38] Wen W, Hsu LT, Zhang G (2018), “Performance Analysis of NDT-based Graph SLAM for Autonomous Vehicle in Diverse Typical Driving Scenarios of Hong Kong,” *Sensors*. 18. 3928. 10.3390/s18113928.
- [39] Wang YT, Peng CC, Ravankar AA, Ravankar A, “A single LiDAR-Based Feature Fusion Indoor Localization Algorithm,” *Sensors*, Vol. 18, 2018, pp. 1294.
- [40] Ravankar A, Ravankar AA, Kobayashi Y, Hoshino Y, Peng CC, “Path Smoothing Techniques in Robot Navigation: State-of-the-Art, Current and Future Challenges,” *Sensors*, Vol. 18, 2018, pp. 3170.
- [41] Peng C, Wang Y, “LIDAR based scan matching for indoor localization,” 2017 IEEE/SICE International Symposium on System Integration (SII), Taipei, 2017, pp. 139-144, doi: 10.1109/SII.2017.8279202.
- [42] Chen L, Peng C, “A Robust 2D-SLAM Technology With Environmental Variation Adaptability,” *Sensors*, Vol. 19, No. 23, 2019, pp. 11475-11491, doi: 10.1109/JSEN.2019.2931368.